Int. J. Contemp. Math. Sci., Vol. 1, 2006, no. 4, 177 - 204

Adaptive Hierarchical Fuzzy Sliding-Mode Control for a Class of Coupling Nonlinear Systems

Chih-Min Lin*, *Senior Member, IEEE*, and Wei-Liang Chin
Department of Electrical Engineering, Yuan-Ze University,
Chung-Li, Tao-Yuan, 320, Taiwan, Republic of China
*Tel: 886-3-4638800 ext 2418
Fax: 886-3-4639355
E-mail: *cml@saturn.yzu.edu.tw*

Abstract: In this paper, an adaptive hierarchical fuzzy sliding-mode control (AHFSMC) for a class of coupling nonlinear systems is derived. The coupling system can be divided into two subsystems, and two sliding surfaces are constructed through the state variables of the coupling systems. An intermediate variable is introduced to incorporate these two sliding surface. Then, an AHFSMC system is designed to simultaneously control the state variables of these two subsystems by

using a single control input. The adaptive laws of the control system are derived in the sense of Lyapunov, so that the control system can be guaranteed to be stable. The proposed control system is then applied to a crane system and a translational oscillator with rotational a actuator system. Simulation results verify that the proposed ADFSMC can drive all the state variables to zero with satisfactory transient responses by using a single control input.

Keywords: hierarchical fuzzy sliding-mode control, Adaptive law, nonlinear coupling systems

I. Introduction

Sliding-mode control (SMC) is a robust design methodology developed by using a systematic scheme based on a sliding surface and Lyapunov's stability theorem [1, 8, 9]. The main advantage of SMC is that the system uncertainties can be handled under the invariance characteristics of system's sliding condition with guaranteed system stability. However, chattering of the control signal is its disadvantage. One approach to

avoid the chattering control signal in SMC is to replace the sign function with a saturation function; however, this will sacrifice for the steady-state tracking accuracy of system responses. Recently, there has been much research on the design of fuzzy logic control (FLC) based on the sliding-mode control scheme, referred to as fuzzy sliding-mode controls (FSMCs) [4, 5, 12]. FSMC has the advantages of both FLC and SMC. It can also reduce chattering of the control system compared to SMC. Moreover, by introducing an intermediate variable, a decoupled fuzzy sliding-mode control design method has been proposed to achieve decoupling performance of a class of nonlinear coupling systems [7]. In [6], a hybrid fuzzy sliding-mode control has been proposed to control an aeroelastic system. However, the decoupled fuzzy sliding-mode control methods presented in [6, 7] have not discussed the stability problem.

In this paper, an adaptive hierarchical fuzzy sliding-mode control (AHFSMC) for a class of coupling nonlinear systems is derived. The coupling system can be divided into two subsystems, and two sliding surfaces are constructed through the state variables of the decoupled

system. An intermediate variable is introduced to incorporate these two sliding surface. Then, an AHFSMC system is designed to simultaneously control the states. The AHFSMC system is comprised of a fuzzy controller and a compensation controller. The fuzzy controller is used to mimic an equivalent controller and the compensation controller is designed to compensate for the approximation error between the fuzzy controller and the equivalent controller. The adaptive laws are derived to tune the parameters of the fuzzy controller and to estimate the error bound of the compensation controller with guaranteed system stability. The proposed control system is then applied to a crane system and a translational oscillator with rotational an actuator system to illustrate its effectiveness.

II. Problem Formulation

Consider a class of coupling nonlinear systems which can be divided into two subsystems as:

$$\begin{aligned} \mathrm{A}: &\begin{cases} \dot{x}_1 = x_2 \\ \dot{x}_2 = f_1(\mathbf{x}) + g_1(\mathbf{x})u \end{cases} \\ \mathrm{B}: &\begin{cases} \dot{x}_3 = x_4 \\ \dot{x}_4 = f_2(\mathbf{x}) + g_2(\mathbf{x})u \end{cases} \end{aligned} \tag{1}$$

According to the definition of the sliding-mode control, define a suitable pair of sliding surfaces as

$$s_1 = \dot{x}_1 + \lambda_1 x_1 = x_2 + \lambda_1 x_1 \tag{2}$$

$$s_2 = \dot{x}_3 + \lambda_2 x_3 = x_4 + \lambda_2 x_3 \tag{3}$$

where λ_1 and λ_2 are positive constants. In (1), the whole system is divided into two subsystems A and B. Then, define a sliding surface of subsystem A which contains the subtarget and sliding surface of subsystem B which contains the main control objective. Define an intermediate variable z, which represents the information from subsystem A, and it is incorporated into s_2. Therefore, the sliding surface s_2 is modified as [7]

$$s_2 = \lambda_2(x_3 - z) + x_4 \tag{4}$$

where the intermediate variable z is related to s_1. Moreover, $\dot{s}_2$ can be calculated as

$$\begin{aligned}\dot{s}_2 &= \lambda_2(\dot{x}_3 - \dot{z}) + \dot{x}_4 \\ &= \lambda_2 x_4 - \lambda_2 \dot{z} + f_2 + g_2 u\end{aligned} \tag{5}$$

In the decoupled sliding surface of (4), the boundedness of x_3 is guaranteed by letting

$$|z| \le \bar{z}, \quad 0 < \bar{z} < 1 \tag{6}$$

where $\bar{z}$ is an upper bound of $|z|$. For the decoupling control, define z as

$$z = \bar{z} \cdot sat(s_1 / \Phi_z) \tag{7}$$

where Φ_z is the boundary layer of s_1 and transfers s_1 to the proper range of x_3; and $sat(\cdot)$ is the saturation function defined as follows:

$$sat(s_1 / \Phi_z) = \begin{cases} \mathrm{sgn}(s_1 / \Phi_z), & \text{if } |s_1 / \Phi_z| \ge 1 \\ s_1 / \Phi_z, & \text{if } |s_1 / \Phi_z| < 1 \end{cases} \tag{8}$$

Since $\bar{z}$ is less than one, z presents a decaying signal. As s_1 decreases, z decreases too. When $s_1 \to 0$, $z \to 0$, $x_3 \to 0$ then $s_2 \to 0$ and the control objective will be achieved. Thus, by the introduction of the intermediate variable z, s_1 and s_2 can be controlled to be reduced to zero at the same time.

By the sliding-mode control, an equivalent controller can be obtained from $\dot{s}_2 = 0$ [8], i.e.

$$u_{eq} = \frac{-\lambda_2 x_4 + \lambda_2 \dot{z} - f_2}{g_2} \tag{9}$$

Because the z function is not differentiable, $\dot{z}$ can not be obtained. Thus, the following adaptive hierarchical fuzzy sliding-mode control is proposed.

III. Adaptive Hierarchical Fuzzy Sliding-Mode Control

Considering the fourth-order system shown in (1), an adaptive hierarchical fuzzy sliding-mode control (AHFSMC) is proposed to control the whole system states to approach to zero with favorable transient responses. Consider the following fuzzy control system for the control input u_f :

$$\text{Rule } i\text{: If } s_2 \text{ is } F_1^i\text{, Then } u_f \text{ is } \theta_i \tag{10}$$

where $F_1^i, i = 1, 2, \cdots, n$ are the labels of the fuzzy sets characterized by the fuzzy membership functions $\mu_{F_1^i}(\cdot)$ and $\theta_i,\ i = 1, 2, \cdots, n$ are the adjustable fuzzy singletons. The defuzzification of the output is accomplished by the method of center-of-gravity

$$u_f = \frac{\sum_{i=1}^{n} \theta_i \times \xi_i}{\sum_{i=1}^{n} \xi_i} = \mathbf{\Theta}^T \boldsymbol{\xi} \tag{11}$$

where $\xi_i = \mu_{F_1^i}(s_2)$ is the firing weight of the i-th rule of (10), $\mathbf{\Theta} = [\theta_1 \quad \theta_2 \quad \cdots \quad \theta_n]^T$ and $\boldsymbol{\xi} = \left[\xi_1 / \sum_{i=1}^{n} \xi_i \quad \xi_2 / \sum_{i=1}^{n} \xi_i \quad \cdots \quad \xi_n / \sum_{i=1}^{n} \xi_i \right]^T$.

By the universal approximation theorem [11], there exists an optimal fuzzy system u_f^* such that

$$u_f^*(s_2, \theta^*) = \mathbf{\Theta}^{*T} \boldsymbol{\xi} \tag{12}$$

where the time invariant optimal parameter vector Θ^* is defined as

$$\mathbf{\Theta}^* = \arg \min_{|\mathbf{\Theta}| \le M_{\mathbf{\Theta}}} \left\{ \sup_{|s_2| \le M_{s_2}} \left| u_f(s_2, \mathbf{\Theta}) - u_{eq} \right| \right\} \quad \text{for all } t \tag{13}$$

and M_{s_2} and $M_{\mathbf{\Theta}}$ are specified by the designer. The minimum approximation error is defined as

$$d(t) = u_f^* - u_{eq}, \qquad 0 \le |d(t)| \le D \tag{14}$$

where the uncertainty bound D is a positive constant. However, this uncertainty bound can not be measured for practical application. Thus, a bound estimation $\hat{D}$ will be developed to estimate the approximation error bound. Define the estimation error $\tilde{D}(t) = D - \hat{D}(t)$, where $\hat{D}(t)$ is the estimated approximation error bound, then the control law is

assumed to take the form:

$$u(s_2, \hat{\theta}, \hat{D}) = u_f(s_2, \hat{\theta}) + u_c(s_2, \hat{D}) \tag{15}$$

where the fuzzy controller u_f given in (11) is used to mimic the equivalent controller in (9); and the compensation controller u_c given in the following is used to compensate for the difference between the equivalent controller and the fuzzy controller.

$$u_C = -\hat{D}\,\mathrm{sgn}(g_2 s_2) \tag{16}$$

The adaptive laws will be developed to adjust the parameters $\hat{\theta}(t)$ and $\hat{D}(t)$ to estimate θ^* and D, respectively.

Substituting (15) into (5) and from (9) and (14), it is obtained that

$$\begin{aligned} \dot{s}_2 &= \lambda_2 x_4 - \lambda_2 \dot{z} + f_2 + g_2(u_f + u_c) \\ &= \lambda_2 x_4 - \lambda_2 \dot{z} + f_2 + g_2(u_f - u_f^* + u_f^* + u_c) \\ &= g_2(u_f - u_f^* + u_c + d) \end{aligned} \tag{17}$$

Then, the following theorem can be stated and proven.

Theorem 1: Consider the nonlinear system presented in (1). The control law is designed as in (15), in which the fuzzy controller u_f is given in (11) with the adaptive law given in (18) and the compensation controller u_c is given in (18) with the bound estimation presented in (19),

$$\dot{\hat{\mathbf{\Theta}}} = -\dot{\tilde{\mathbf{\Theta}}} = \eta_1 g_2 s_2 \xi \tag{18}$$

$$\dot{\hat{D}} = -\dot{\tilde{D}} = \eta_2 \left| g_2 s_2 \right| \tag{19}$$

where η_1 and η_2 are positive constants. Then, the stability of the system can be guaranteed.

Proof: Define a Lyapunov function as

$$V(s_2, \tilde{\mathbf{\Theta}}, \tilde{D}) = \frac{1}{2} s_2^{\,2} + \frac{1}{2\eta_1} \tilde{\mathbf{\Theta}}^T \tilde{\mathbf{\Theta}} + \frac{1}{2\eta_2} \tilde{D}^2 \tag{20}$$

where $\tilde{\mathbf{\Theta}} = \mathbf{\Theta}^* - \hat{\mathbf{\Theta}}$. When (20) is differentiated with respect to time, and by the use of (11), (14), (16) and (17), it is obtained that

$$\begin{aligned}
\dot{V}(s_2, \tilde{\mathbf{\Theta}}, \tilde{K}) &= s_2 \dot{s}_2 + \frac{1}{\eta_1} \tilde{\mathbf{\Theta}}^T \dot{\tilde{\mathbf{\Theta}}} + \frac{1}{\eta_2} \tilde{D} \dot{\tilde{D}} \\
&= g_2 s_2 (u_f - u_f^{\,*} + u_c + d) + \frac{1}{\eta_1} \tilde{\mathbf{\Theta}}^T \dot{\tilde{\mathbf{\Theta}}} - (D - \hat{D}) \left| g_2 s_2 \right| \\
&= g_2 s_2 (\tilde{\mathbf{\Theta}}^T \xi - \hat{D} \operatorname{sgn}(g_2 s_2) + d) + \frac{1}{\eta_1} \tilde{\mathbf{\Theta}}^T \dot{\tilde{\mathbf{\Theta}}} - D \left| g_2 s_2 \right| + \hat{D} \left| g_2 s_2 \right| \\
&= \frac{1}{\eta_1} \tilde{\mathbf{\Theta}}^T (\eta_1 g_2 s_2 \xi + \dot{\tilde{\mathbf{\Theta}}}) - \hat{D} \left| g_2 s_2 \right| + d g_2 s_2 - D \left| g_2 s_2 \right| + \hat{D} \left| g_2 s_2 \right| \\
&= d g_2 s_2 - D \left| g_2 s_2 \right| \\
&\le 0
\end{aligned}$$

(21)

The negative semidefiniteness of the Lyapunov function guarantees that s_2, $\hat{\mathbf{\Theta}}$ and $\hat{D}$ are bounded. Let $L(t) = -d g_2 s_2 \;\le\; -\dot{V}(s_2, \tilde{\mathbf{\Theta}}, \tilde{D})$

and integrate $L(t)$ with respect to time, then yields

$$\int_0^t L(\tau)d\tau \le V(s_2(0),\tilde{\mathbf{\Theta}}(0),\tilde{D}(0)) - V(s_2(t),\tilde{\mathbf{\Theta}}(t),\tilde{D}(t)) \tag{22}$$

Because $V(s_2(0),\tilde{\mathbf{\Theta}}(0),\tilde{D}(0))$ is bounded, and $V(s_2(t),\tilde{\mathbf{\Theta}}(t),\tilde{D}(t))$ is nonincreasing and bounded, it is shown that

$$\lim_{t\to\infty}\int_0^t L(\tau)d\tau < \infty \tag{23}$$

In addition, since $\dot{L}(t)$ is bounded, by the Barbalat's lemma [8], it can be shown that $\lim_{t\to\infty} L(t) = 0$. That is $s_2(t) \to 0$ as $t \to \infty$. Moreover, as discussed in section II, $s_1(t) \to 0$ as $t \to \infty$ can be also achieved. As a result, the control system is asympatoically stable. Thus, the proof of *Theorem 1* is complete.

IV. Simulation Result

In this section, the proposed adaptive hierarchical fuzzy sliding-mode controller is applied to an overhead crane system and a translational oscillator with rotational actuator (TORA) system to illustrate its effectiveness. It should be emphasized that the derivation of the proposed AHFSMC does not need to use the dynamic functions $f_1(\mathbf{x})$,

$f_2(\mathbf{x})$, $g_1(\mathbf{x})$ and $g_2(\mathbf{x})$ in (1). These dynamic functions are used only for simulations. This is the best advantage of the proposed control method than a lot of nonlinear control methods [2, 3, 10]

(a) Overhead crane system control

The structure and controlled states of the overhead crane system are shown in Fig.1 [10]. The trolley having a mass M on x-direction rail is driven by a force f . The load having a mass m is suspended from the trolley by a rigid rope.

For simplicity, the following assumptions are made:

(A) The trolley and the load can be regarded as point mass;

(B) Friction force in the trolley can be neglected;

(C) Elongation of the rope due to tension force is neglected;

(D) The trolley moves always in x direction;

(E) The load moves always in x-y surface.

The dynamics of this crane system can be represented as (1), where

$$
\begin{aligned}
f_1(\mathbf{x}) &= \frac{mLx_4{}^2 \sin x_3 + mg \sin x_3 \cos x_3}{M + m\sin^2 x_3} \\
f_2(\mathbf{x}) &= -\frac{(m+M)g \sin x_3 + mLx_4{}^2 \sin x_3 \cos x_3}{(M + m\sin^2 x_3)^2 L} \\
g_1(\mathbf{x}) &= \frac{1}{M + m\sin^2 x_3} \\
g_2(\mathbf{x}) &= -\frac{1}{(M + m\sin^2 x_3)L}
\end{aligned}
\tag{24}
$$

The derivation of the overhead crane system is given in **Appendix A**. In the simulations, the parameters are chosen as $M = 1\,\text{Kg}$, $m = 0.8\,\text{Kg}$; $L = 0.305\,\text{m}$ and g =9.8. The used parameters in (7) are $\bar{z} = 0.99$ and $\Phi_z = 5$, and the membership functions are constructed for the antecedent part; the value of the center of the triangular-type membership functions are given as $[-3.5 \quad -1.5 \quad -0.5 \quad 0 \quad 0.5 \quad 1.5 \quad 3.5]$. The slope of the sliding surfaces s_1 and s_2 are $\lambda_1 = 0.6$ and $\lambda_2 = 100$, respectively. The learning-rate of the adaptive law and the estimation law in (18) and (19) are $\eta_1 = 30$ and $\eta_2 = 0.001$. These parameters are chosen trough some trials.

For the initial conditions $x_1 = -2$ m, $x_2 = 0$ m/s, $x_3 = 0$ rad and $x_4 = 0$ rad/s, the simulation results for the AHFSMC are shown in Fig. 2.

The simulation results show that, by using the AHFSMC, all states converge to zero with satisfactory control performance.

(b) Translational oscillator with rotational actuator (TORA) system control

The TORA system combines a translational oscillator with an eccentric rotational proof-mass actuator [2, 3]. As shown in Fig. 3, the oscillator consists of a cart connected to a fixed wall by a linear spring. The cart is constrained to move in the x-direction only and all motions occur on a horizontal plane, so no gravitational forces need to be considered. On the platform a rotating eccentric mass is actuated by a dc motor. Its motion applies a force to the platform which can be used to damp the translational oscillations. The proof-mass actuator is attached to the cart and is controlled using an applied torque N. A disturbance force F perturbs the cart. The detail description of the TORA system is given in **Appendix B**. Thus, the equations of the motion can be written as (1), where

$$
\begin{aligned}
f_1(\mathbf{x}) &= -x_1 + \varepsilon \sin x_3 + F_d \\
f_2(\mathbf{x}) &= \frac{\varepsilon \cos x_3 \left[x_1 - \varepsilon \left(1 + x_4{}^2\right) \sin x_3 - F_d \right]}{1 - \varepsilon^2 \cos^2 x_3} \\
g_1(\mathbf{x}) &= 0 \\
g_2(\mathbf{x}) &= \frac{1}{1 - \varepsilon^2 \cos^2 x_3}
\end{aligned}
\tag{25}
$$

In the simulations, the parameters are chosen as $\varepsilon = 0.2$, $\lambda_1 = 20$, $\lambda_2 = 0.5$, $\eta_1 = 1$ and $\eta_2 = 0.001$. These parameters are also chosen trough some trials. The membership functions are set to be the same as the previous subsection.The initial condition is chosen as $\mathbf{x}(0) = \begin{bmatrix} 1 & 1 & 1 & 1 \end{bmatrix}$. The simulation results by using the AHFSMC are shown in Fig. 4. The simulation results also show that all states converge to zero with satisfactory control performance.

V. Conclusion

An adaptive hierarchical fuzzy sliding-mode control (AHFSMC) of a class of coupling nonlinear system is presented. The idea behind the control law is as follows. First, the coupling system is divided into two subsystems; and each subsystem has a separate control target expressed in terms of a sliding surface. An intermediate variable is introduced to

incorporate these sliding surfaces. Then, design the AHFSMC system such that a single control input can simultaneously drive all the states to converge to zero with guaranteed system stability and satisfactory transient responses. The best advantage of the proposed design method is that it does not need to know the system dynamics of the controlled system. Simulation results have verified the effectiveness of the proposed design method.

Appendix A: Derivation of the overhead crane system [10]

From Fig. 1 we can find that $x_m = x + L\sin\theta$, $y_m = -L\cos\theta$, where L is the length of the suspension rope and θ is the swing angle of the load.

The kinetic energy is represented by

$$T = \frac{1}{2}M\dot{x}^2 + \frac{1}{2}m\left(\dot{x}_m{}^2 + \dot{y}_m{}^2\right) \tag{A1}$$

The potential energy is also represented by

$$H = mgy_m = -mgL\cos\theta \tag{A2}$$

where g is the gravitational acceleration. The Lagrangian function

$\tilde{L} = T - H$ is obtained as:

$$\tilde{L} = T - H = \frac{1}{2}M\dot{x}^2 + \frac{1}{2}m\left(\dot{x}^2 + L^2\dot{\theta}^2 + 2\dot{x}\dot{\theta}L\cos\theta\right) + mgL\cos\theta \tag{A3}$$

Now, we use the general form of Lagrange's equations with a Lagrange multiplier. With Lagrange's equations

$$\frac{d}{dt}\left(\frac{\partial\hat{L}}{\partial\dot{q}}\right) - \frac{\partial\hat{L}}{\partial q} = Q \tag{A4}$$

The equations of motion associated with the generalized coordinates $q = \begin{bmatrix} x & \theta \end{bmatrix}^T$ are presented. From the Lagrange's equation (A4). We formulate the relation:

$$\begin{aligned} &\frac{d}{dx}\left(\frac{\partial\tilde{L}}{\partial\dot{\theta}}\right) - \frac{\partial\tilde{L}}{\partial\theta} = 0 \\ &\frac{d}{dx}\left(\frac{\partial\tilde{L}}{\partial\dot{x}}\right) - \frac{\partial\tilde{L}}{\partial x} = f \end{aligned} \tag{A5}$$

According to the Lagrange's equations, we can obtain the following equations related to the generalized coordinates x, θ, respectively, as

$$\begin{aligned} &x : (m+M)\ddot{x} + mL\left(\ddot{\theta}\cos\theta - \dot{\theta}^2\sin\theta\right) = f \\ &\theta : \ddot{x}\cos\theta + L\ddot{\theta} + g\sin\theta = 0 \end{aligned} \tag{A6}$$

In summary, we can obtain $f_1(\mathbf{x})$, $f_2(\mathbf{x})$, $g_1(\mathbf{x})$, $g_2(\mathbf{x})$ in (1) as

$$
\begin{aligned}
f_1(\mathbf{x}) &= \frac{mL\dot{\theta}^2 \sin\theta + mg\sin\theta\cos\theta}{M + m\sin^2\theta} \\
f_2(\mathbf{x}) &= -\frac{(m+M)g\sin\theta + mL\dot{\theta}^2\sin\theta\cos\theta}{(M + m\sin^2\theta)^2 L} \\
g_1(\mathbf{x}) &= \frac{1}{M + m\sin^2\theta} \\
g_2(\mathbf{x}) &= -\frac{1}{(M + m\sin^2\theta)L}
\end{aligned}
\tag{A7}
$$

Appendix B: Translational oscillator with rotational actuator (TORA) system [2, 3]

System parameters

$M = 1.3608$ kg cart mass;

$m = 0.096$ kg Arm mass;

$e = 0.0592$ m Arm eccentricity;

$I = 0.0002175$ kg m^2 Arm inertia;

$k = 186.3$ N/m Spring stiffness;

The equations of motion are given by

$$
\begin{aligned}
(M+m)x_c + kx_c &= -me(\ddot{\theta}\cos\theta - \dot{\theta}^2\sin\theta) + F \\
(I + me^2)\ddot{\theta} &= -me\ddot{x}_c\cos\theta + N
\end{aligned}
\tag{B.1}
$$

Defining the normalized variables

$$\begin{aligned}
\xi &= \sqrt{\frac{M+m}{I+me^2}}x_c \\
u &= \frac{M+m}{k(I+me^2)}N \\
\tau &= \sqrt{\frac{k}{M+m}}t \\
\omega &= \frac{1}{k}\sqrt{\frac{M+m}{I+me^2}}F
\end{aligned} \tag{B.2}$$

the equations of motion (B.1) become

$$\begin{aligned}
\ddot{\xi} + \xi &= \varepsilon(\dot{\theta}^2 \sin\theta - \ddot{\theta}\cos\theta) + \omega \\
\ddot{\theta} &= -\varepsilon\ddot{\xi}\cos\theta + u
\end{aligned} \tag{B.3}$$

where ξ is the normalized cart position, and ω and u represent the non-dimensionalized disturbance and control torque, respectively. In the normalized equations, the dot means differentiation with respect to the normalized time τ. The coupling between the translational and rotational motions is represented by the parameter ε which is defined by

$$\varepsilon = \frac{me}{\sqrt{(I+me^2)(M+m)}} = 0.2 \tag{B.4}$$

By defining $\mathbf{x} = \begin{bmatrix} \xi & \dot{\xi} & \theta & \dot{\theta} \end{bmatrix}$, the system is written in the form as

$$\dot{\mathbf{x}} = F(\mathbf{x}) + G(\mathbf{x})u + D(\mathbf{x})\omega \tag{B.5}$$

The vectors $F(\mathbf{x})$, $G(\mathbf{x})$ and $D(\mathbf{x})$ are given by

$$F(\mathbf{x}) = \begin{bmatrix} \dot{x}_c \\ \dfrac{-x_c + \varepsilon\dot{\theta}^2 \sin\theta}{1-\varepsilon^2\cos^2\theta} \\ \dot{\theta} \\ \dfrac{\varepsilon\cos\theta(x_c - \varepsilon\dot{\theta}^2\sin\theta)}{1-\varepsilon^2\cos^2\theta} \end{bmatrix}$$

$$G(\mathbf{x}) = \begin{bmatrix} 0 \\ \dfrac{-\varepsilon\cos\theta}{1-\varepsilon^2\cos^2\theta} \\ 0 \\ \dfrac{1}{1-\varepsilon^2\cos^2\theta} \end{bmatrix}$$

$$D(\mathbf{x}) = \begin{bmatrix} 0 \\ \dfrac{1}{1-\varepsilon^2\cos^2\theta} \\ 0 \\ \dfrac{-\varepsilon\cos\theta}{1-\varepsilon^2\cos^2\theta} \end{bmatrix} \tag{B.6}$$

Let the new state variables

$$\begin{aligned} x_1 &= \xi + \varepsilon\sin\theta \\ x_2 &= \dot{\xi} + \varepsilon\dot{\theta}\cos\theta \\ x_3 &= \theta \\ x_4 &= \dot{\theta} \end{aligned} \tag{B.7}$$

Transforming the system (B.5) into the form as (1), yields

$$\begin{aligned} \dot{x}_1 &= x_2 \\ \dot{x}_2 &= -x_1 + \varepsilon\sin x_3 + F_d \\ \dot{x}_3 &= x_4 \\ \dot{x}_4 &= \frac{\varepsilon\cos x_3\left[x_1 - \varepsilon\left(1+x_4{}^2\right)\sin x_3 - F_d\right]}{1-\varepsilon^2\cos^2 x_3} + \frac{1}{1-\varepsilon^2\cos^2 x_3}u \end{aligned} \tag{B.8}$$

Reference

[1] K. J. Åström and B. Wittenmark, Adaptive Control, New York: Addison-Wesley, 1995.

[2] R. T. Bupp, D. S. Bernstein, and V. T. Coppola, A benchmark problem for nonlinear control design, International Journal of Robust and Nonlinear Control, **8** (1998), 307-310.

[3] M. Jankovic, D. Fontaine, and P. V. Kokotović, TORA example: cascade and passivity-based control designs, IEEE Trans. Control Systems Technology, **4** (1996), 292-297.

[4] C. M. Lin, and C. F. Hsu, Guidance law design by adaptive fuzzy sliding-mode control, Journal of Guidance, Control, and Dynamics, **25** (2002), 248-256.

[5] C. M. Lin, and C. F. Hsu, Adaptive fuzzy sliding-mode control for induction servomotor systems, IEEE Trans. Energy Coversion, **19 (**2004), 362-368.

[6] C. M. Lin, and C. F. Hsu, Hybrid fuzzy sliding-mode control of an aeroelastic system, Journal of Guidance, Control, and Dynamics,

25 (2002), 829-832.

[7] J. C. Lo and Y. H. Kuo, Decoupled fuzzy sliding-mode control, IEEE Trans. Fuzzy Systems, **6** (1998), 426-435.

[8] J. J. E. Slotine and W. Li, Applied Nonlinear Control, Englewood Cliffs, NJ: Prentice-Hall, 1991.

[9] V. I. Utkin, Sliding Modes in Control and Optimization, New York: Springer-Verlag, 1992.

[10] W. Wang, J. Yi, D. Zhao, and X. Liu, Incremental neural network sliding mode controller for an overhead crane, Intelligent Mechatronics and Automation, (2004), 166-171.

[11] L. X. Wang, Adaptive Fuzzy Systems and Control: Design and Stability Analysis, Englewood Cliffs, NJ: Prentice-Hall, 1994.

[12] X. Yu, Z. Man and B. Wu, Design of fuzzy sliding-mode control systems, Fuzzy Sets and Systems, **95 (**1998), 295-306.

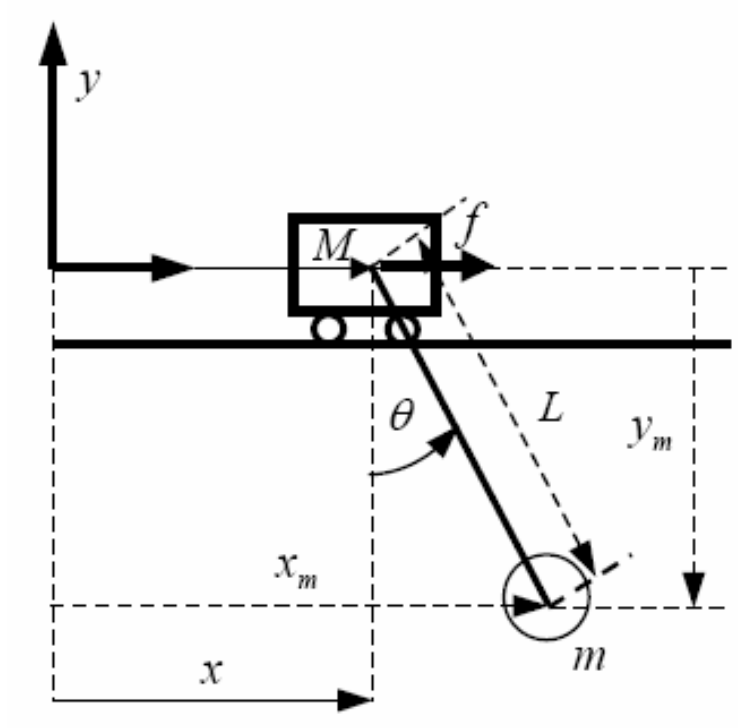

Fig. 1 Structure model of overhead crane system

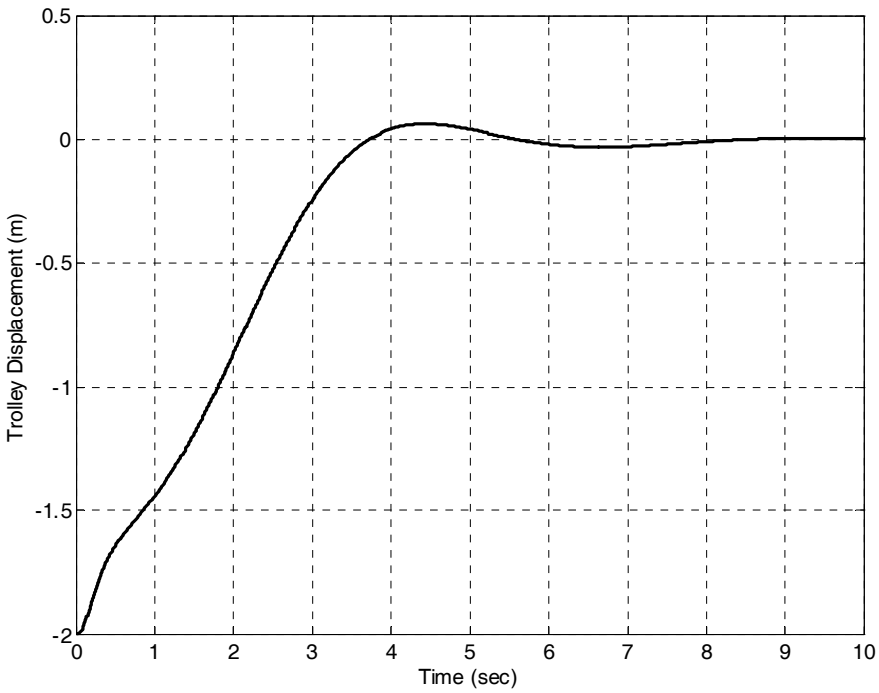

Fig. 2 (a) The trolley displacement response

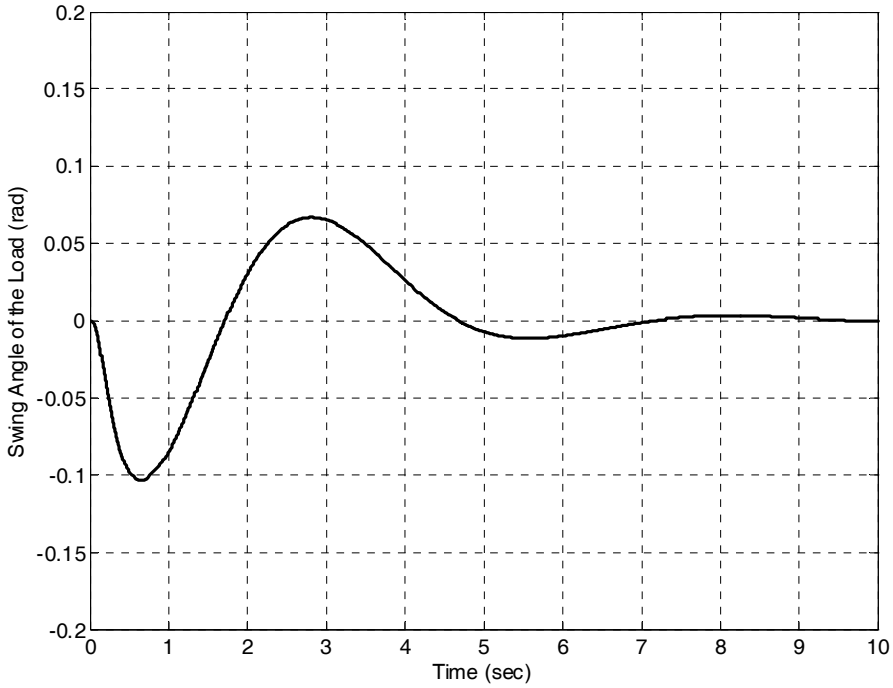

Fig. 2 (b) The swing angle response

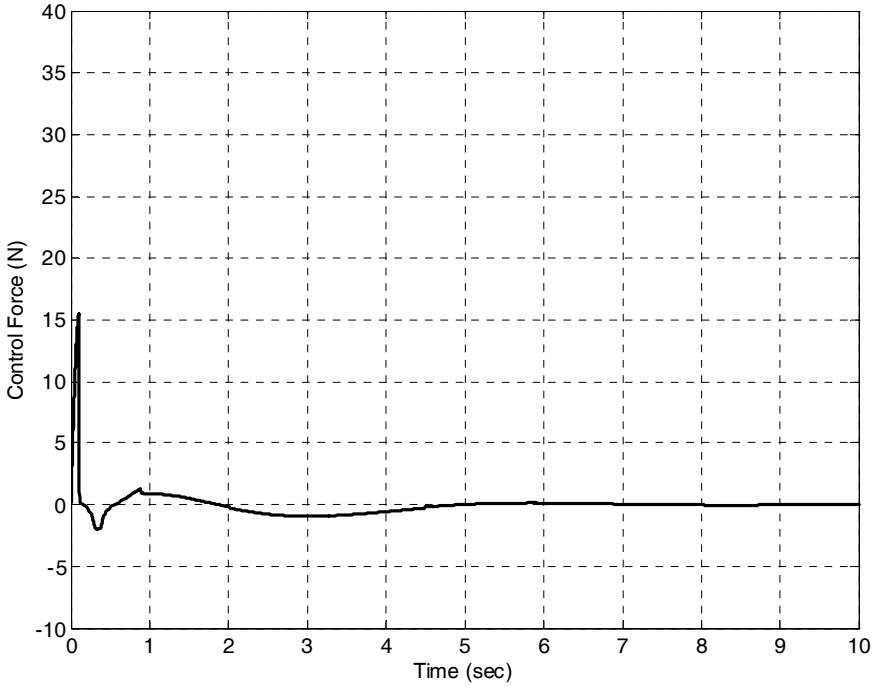

Fig. 2 (c) The control force input

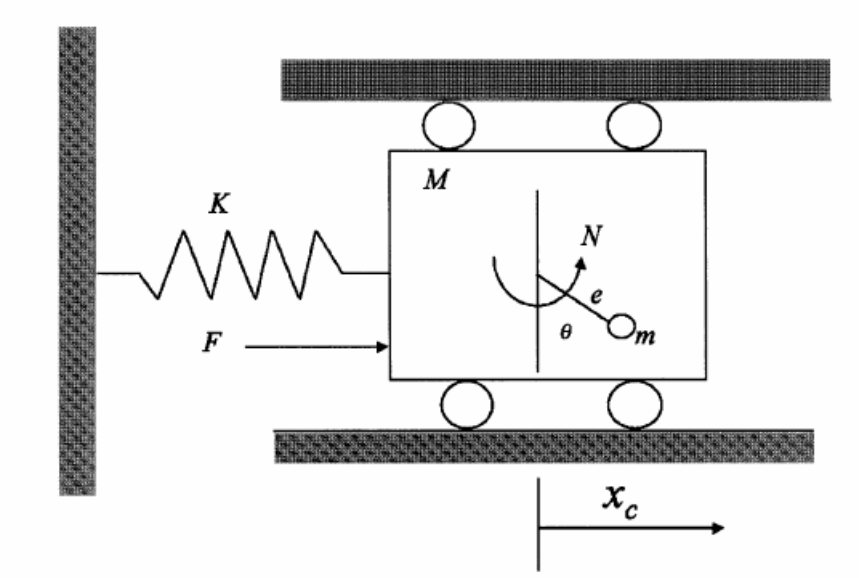

Fig. 3 Translational oscillator with rotational actuator (TORA) system

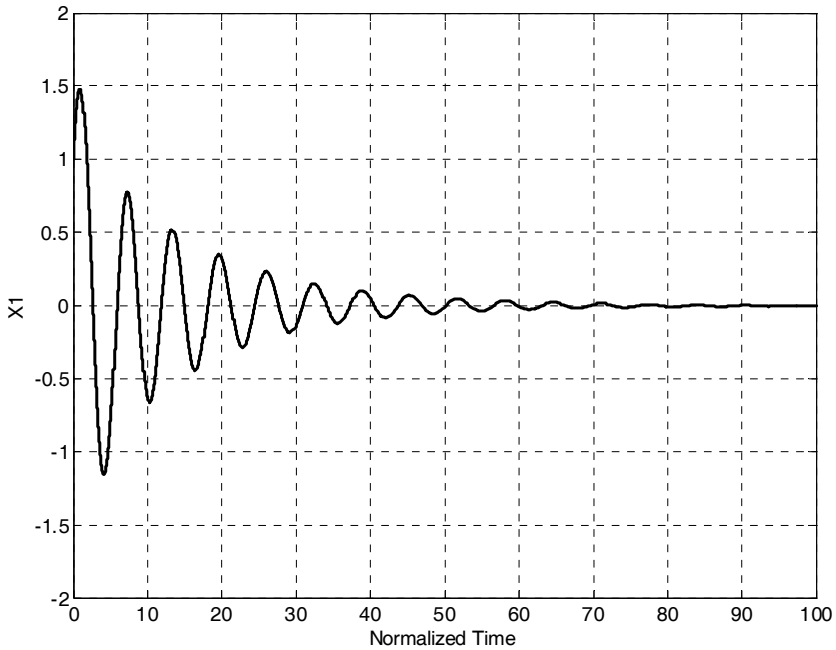

Fig. 4 (a) The normalized state variable x_1

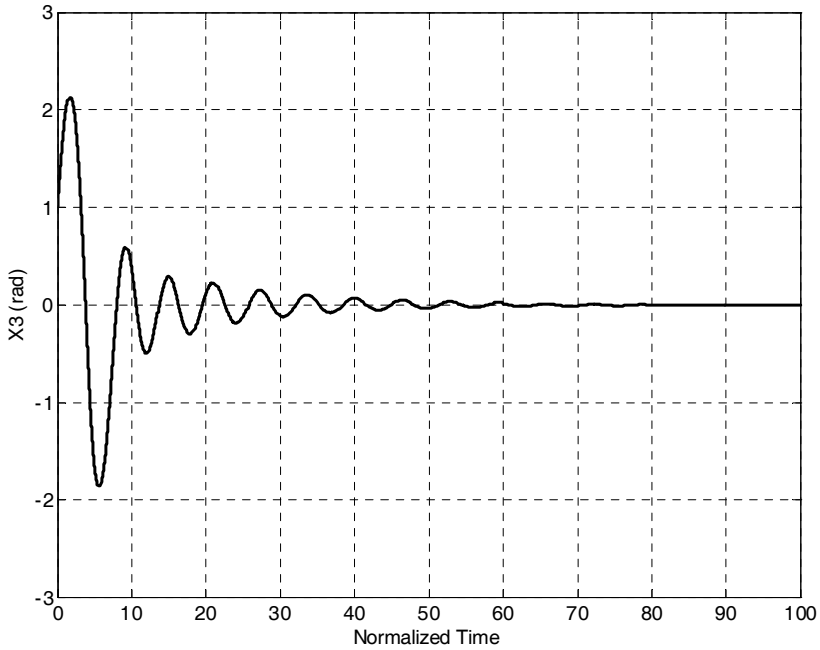

Fig. 4 (b) The angle response

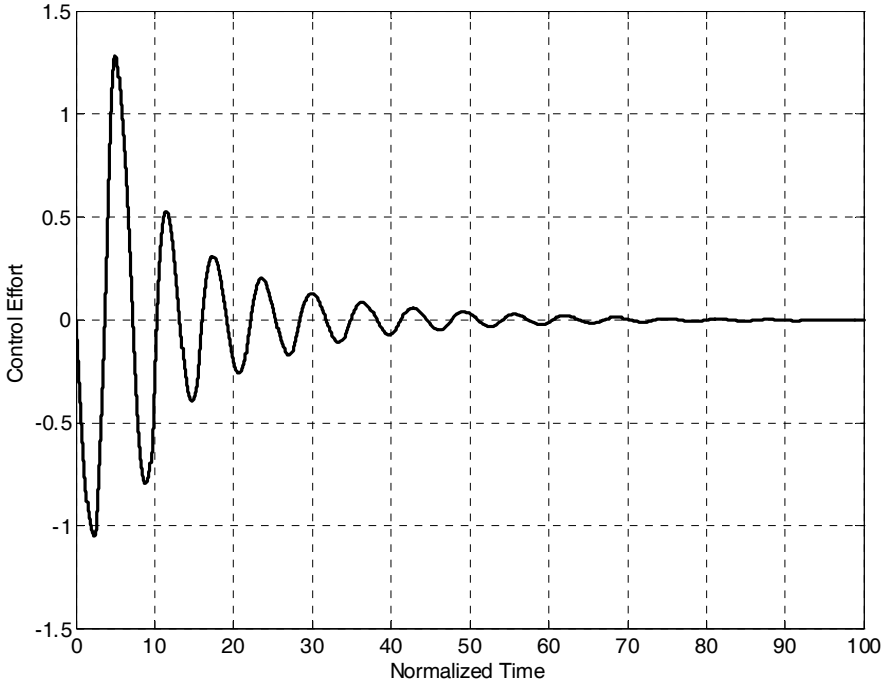

Fig. 4 (c) The control effort

Received: October 21, 2005